APCOM'07 in conjunction with EPMESC XI, *December 3-6, 2007, Kyoto, JAPAN*

Phase-Field Simulations during Dynamic Recrystallization

Y. Hisakuni[1]*, T. Takaki[2], Y. Tomia[1]

[1] *Graduate School of Engineering, Kobe University, 1-1, Rokkoudai, Nada, Kobe, 657-8501, Japan*
[2] *Graduate School of Maritime Sciences, Kobe University, 5-1-1, Fukaeminami, Higashinada, Kobe, 658-0022, Japan*
e-mail: hisakuni@solid.mech.kobe-u.ac.jp , takaki@maritime.kobe-u.ac.jp , tomita@mech.kobe-u.ac.jp .

Abstract When a low-to-medium stacking fault energy (SFE) metal is deformed under a high-temperature environment, dynamic recrystallization (DRX) occurs. DRX is a very complicated phenomenon that involves both hardening due to the accumulation of dislocations and softening due to the nucleation and growth of recrystallized grains. In other words, the mechanical behavior during DRX is closely associated with the evolution of microstructures and dislocations. In our previous study, we developed a phase-field model that can simulate microstructural evolution during DRX. In the model, dislocation evolution and the nucleation of recrystallized grains are predicted theoretically, and the growth of recrystallized grains is simulated by a multi-phase-field method. In this study, through a series of DRX simulations employing the phase-field model developed, we investigate the effects of initial grain size and inhomogeneous deformation on DRX behavior, microstructural evolution and macroscopic stress-strain relationship.

Key words: Phase-Field Method, Dynamic Recrystallization, Microstructural Evolution, Dislocation.

INTRODUCTION

In hot working, a metal undergoes deformation and dynamic restoration simultaneously. The predominant dynamic restoration process, i.e., dynamic recovery or dynamic recrystallization, strongly depends on the magnitude of the stacking fault energy (SFE) of the metal. Because the extended dislocation is slow in a dislocation structure rearranged during dynamic recovery, in a low-to-medium-SFE metal, dislocations accumulate and DRX occurs when dislocation density reaches a critical value. On the other hand, in a high-SFE metal, since dynamic recovery occurs easily, dislocation density does not reach a critical value from which DRX starts.

In DRX process, characteristic stress-strain curves depending on microstructural evolution are observed. Figure 1 schematically shows typical stress-strain curves obtained during DRX, which are characterized by temperature and strain rate, or the Zener-Holloman parameter. At high temperatures and low strain rates, a multiple-peak curve, which is caused by periodic recrystallization cycles with no overlap, is observed. At low temperatures and high strain rates, a single-peak curve appears. In this case, periodic recrystallization cycles overlap and steady-state-flow stress is achieved by the balance between hardening and softening. As mentioned above, the mechanical behavior in hot working is closely associated with microstructural evolution.

To appropriately design the working conditions and control the final microstructures in hot working, numerical investigations are essential. In our previous study [1], we developed a numerical model for predicting microstructural evolution in hot working. In this model, we employed a phase-field method instead of the cellular automaton method of Ding and Guo [2] to simulate the softening caused by recrystallized grain growth, because a phase-field method can accurately account for the curvature effect,

which is an important concern in the grain growth problem. The work hardening model and nucleation criteria followed the models of Ding and Guo [2]. In this study, by performing a series of DRX simulations employing the phase-field model developed, we investigate the effects of initial grain size and inhomogeneous deformation on DRX behavior, microstructural evolution and macroscopic stress-strain curves.

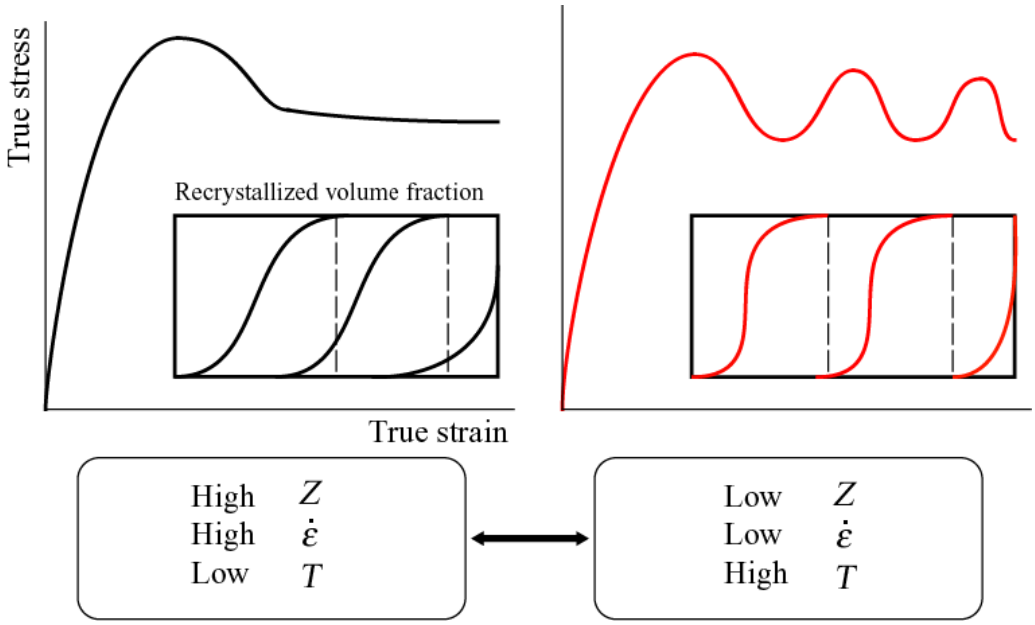

Fig. 1 Schematic stress-strain curves and recrystallized volume fractions.

NUMERICAL MODEL

In this chapter, the numerical model and procedure reported in Ref. [1] are briefly explained. In the model, work hardening and the nucleation of recrystallized grains are modeled theoretically and recrystallized grain growth is reproduced by a multi-phase-field method.

1. Dislocation evolution model We assume that the evolution of dislocation density ρ follows the Kocks and Meching model [3] expressed by

$$\frac{d\rho}{d\varepsilon} = k_1\sqrt{\rho} - k_2\rho, \tag{1}$$

where k_1 is a constant and k_2 is a function of temperature and strain. The flow stress σ is related to the dislocation density by Bailey-Hirsch equation [3] expressed as

$$\sigma = \alpha\mu\tilde{b}\sqrt{\rho}, \tag{2}$$

where α is a constant equal to 0.5, μ is the shear modulus, and $\tilde{b}$ is the magnitude of Burger's vector. We can obtain the stress-strain relation from Eqs. 1 and 2 as

$$\frac{d\sigma}{d\varepsilon} = A(1 - B\sigma), \tag{3}$$

where

$$A = \frac{1}{2}\alpha\mu\tilde{b}k_1, \quad B = \frac{1}{\sigma_s} = \frac{k_2}{\alpha\mu\tilde{b}k_1}.$$

We can determine k_1 as a gradient at $\sigma = 0$ of the stress-strain curve obtained by experiment. The stress σ_s is the steady-state stress without the DRX and determined using [4]

$$\sigma_s = \left[\frac{\dot{\varepsilon}}{A_0} \exp\left(\frac{Q_{act}}{RT} \right) \right]^{1/n'}, \tag{4}$$

where, A_0 and n' are constants, Q_{act} is activation energy, R is gas constant, and T is temperature.

2. Nucleation model Although some nucleation mechanisms of DRX are reported, we assume that the recrystallized grains nucleate by the bulging of existing high grain boundaries. Following Ref. [5], the critical dislocation density ρ_c for creating the nuclei is evaluated using

$$\rho_c = \left(\frac{20\gamma\dot{\varepsilon}}{3\tilde{b}LM\tau} \right)^{1/3}, \tag{5}$$

where M is the grain boundary mobility, τ is the dislocation line energy, L is the mean free pass of dislocation and γ is the grain boundary energy. M, τ and L are expressed as

$$M = M_0 \left(-\frac{Q_b}{RT} \right), \quad \tau = c_2 \mu \tilde{b}^2, \text{ and } \quad L = \frac{K}{\alpha\sqrt{\rho}}, \tag{6}$$

where M_0 is the pre-exponential factor, Q_b is the activation energy, c_2 is a constant equal to 0.5, and K is a constant that is about 10 for most metals.

We assume nucleation rate to be a function of temperature and strain rate, and we employ

$$\dot{n} = c\dot{\varepsilon} \exp\left(-\frac{Q_{act}}{RT} \right), \tag{7}$$

where c is a constant.

3. Phase-field model We use the multi-phase-field model of Steinbach et al. [6]. The phase field ϕ_i takes a value of 1 inside the i-th grain, 0 inside the other grains, and $0 < \phi_i < 1$ at the grain boundary. The phase field ϕ_i is not an independent variable and must satisfy $\sum_{i=1}^{n} \phi_i = 1$. The time evolution equations for phase field ϕ_i are given by

$$\dot{\phi}_i = -\sum_{j=1}^{n} \frac{M_{ij}^{\phi}}{n} \left[\sum_{k=1}^{n} \left\{ \left(W_{ik} - W_{jk} \right) \phi_k + \frac{1}{2} \left(a_{ik}^2 - a_{jk}^2 \right) \nabla^2 \phi_k \right\} - \frac{8}{\pi} \sqrt{\phi_i \phi_j} \Delta E_{ij} \right], \tag{8}$$

where n is the number of interface fields on a numerical grid point. a_{ij}, W_{ij}, and M^{ϕ}_{ij} are the gradient coefficient, barrier height and phase field mobility, respectively, and are related to the interface energy γ_{ij}, the grain boundary thickness δ, and the grain boundary mobility M_{ij} through

$$a_{ij} = \frac{2}{\pi}\sqrt{2\delta\gamma_{ij}}, \quad W_{ij} = \frac{4\gamma_{ij}}{\delta}, \text{ and } \quad M_{ij}^{\phi} = \frac{\pi^2}{4\delta} M_{ij}. \tag{9}$$

ΔE_{ij} is the driving force, or the stored energy, between the i-th and j-th grains and is calculated from the difference in dislocation density using

$$\Delta E_{ij} = \tau(\rho_j - \rho_i),$$

where ρ_i and ρ_j are dislocation densities that uniformly distribute inside the i-th and j-th grains, respectively. The profiles of phase field and dislocation density in one dimension are schematically shown in Fig. 2.

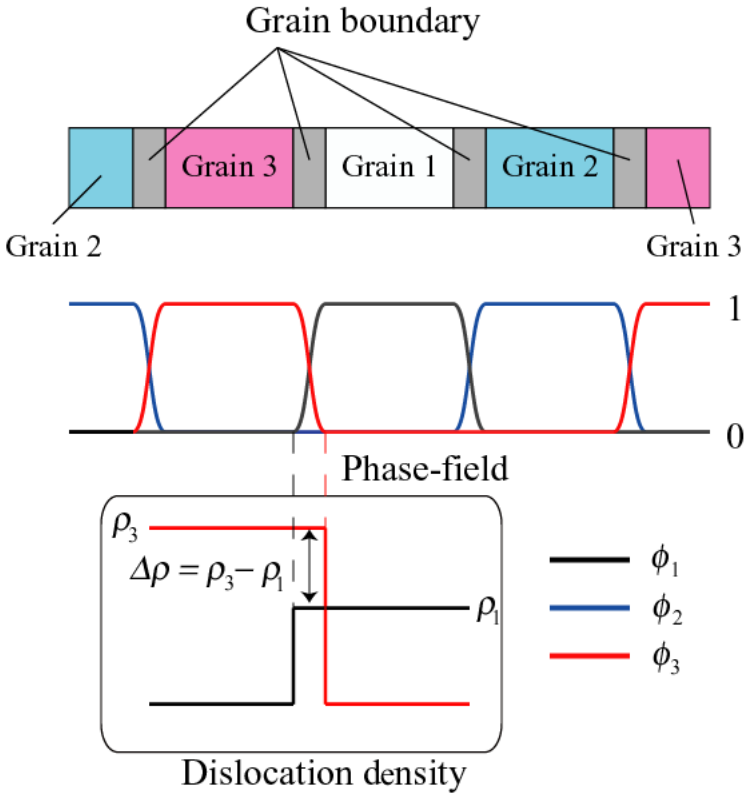

Fig. 2 Schematic illustration of profiles of phase field and dislocation density.

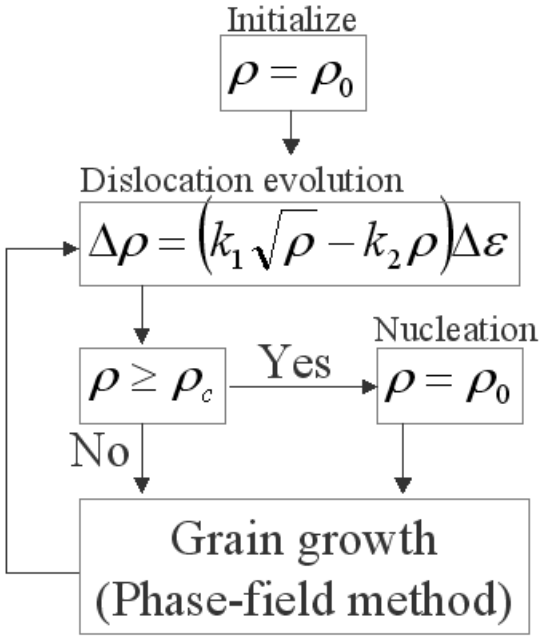

Fig. 3 Numerical procedure for DRX.

4. Numerical procedure Figure 3 shows the numerical procedure during DRX. The finite difference method is used to solve Eq. 8. First, the dislocation densities at all grid points are initialized to their initial values ρ_0. Second, the new dislocation densities corresponding to the strain increment $\Delta\varepsilon$ are calculated using Eq. 1. Third, if the dislocation density at the high-angle grain boundary reaches the critical value

calculated using Eq. 5, and the present time step becomes the step corresponding to the nucleation rate of Eq. 7, the nucleus is put on the grid point. Here, the dislocation density inside the new nucleus is set to the initial value. Fourth, the grain growth driven by the stored energy is simulated by solving Eq. 8. These steps are repeated until a predetermined strain is reached. The macroscopic stress-strain relationship is obtained by substituting the average dislocation density in Eq. 2.

NUMERICAL CONDITIONS

DRX simulations are carried out in the square computational domain of 200×200 μm (400×400 lattices) and the lattice size $\Delta x = \Delta y = 0.2$ μm subjected to periodic boundary conditions. Oxygen-free high conductivity (OFHC) copper is selected as the test material. The material parameters used in this study are listed in Table 1. The temperature and strain rate are set to be 775 K and 2.0×10^{-3} s^{-1}, respectively, and the material is deformed up to the true strain of 1.0. The initial grain structures are prepared by normal grain growth simulation from nuclei generated randomly. As mentioned before, since the driving force of DRX is very small, nuclei of DRX are formed by the bulging of the present grain boundary, the formation of twin boundary, the sliding of the grain boundary and so on. However, since the present model cannot consider the winding or serration of the grain boundary, the critical radius of the nucleus, r_c, is determined by the balance between the grain boundary energy γ and the driving force ΔE, i.e. $r_c = 2\gamma/\Delta E$. In this case, the calculated radius of the nucleus becomes very large. Therefore, in order to reduce the critical radius of the nucleus, we set $\Delta E_{ij} = 4\ \Delta E_{ij}$ and $M^{\phi}_{ij} = 1/4 M^{\phi}_{ij}$.

Table.1 Materials and computational parameters.

k_1, k_2	521×10^{6} [1/m], 40.2	μ	4.21×10^{10} [Pa]
$\tilde{b}$	2.5610-10 [m]	A_0	2.78×10^{-45}
Q_{act}	261 [kJ/mol]	R	8.314 [J/mol K]
n'	7.58	M_0	1.25×10^{-15} [m^3/s]
Q_b	104 [kJ/mol]	c	5.0×10^{23}
τ	5.39 [J/m]	γ	0.625[J/m^2]
ρ_0	1.0×10^{9} [$1/m^2$]		

NUMERICAL RESULTS AND DISCUSSION

1. Effects of initial grain size To investigate the effects of initial grain size on microstructual evolution and macroscopic stress-strain relationship, grain structures with average grain sizes D_0 = 24, 30 and 43 μm are prepared before the DRX simulation. Figure 4 shows the calculated stress-strain curves. Since the critical dislocation density is $\rho_c = 1.54\times10^{14}$ $1/m^2$ from Eq. 5, the corresponding stress is calculated to be σ = 66.8 MPa using Eq. 2. The stresses reach maximum at approximately ε = 0.17 for all D_0 values. The maximum stress is higher for a larger initial grain. Although a similar tendency is observed in the experimental results, the differences between the maximum stresses are very small compared with those observed by the experiment [4]. By reaching the maximum stress point, the softening due to the nucleation and growth of recrystallized grains becomes predominant, as compared with the hardening by dislocation accumulation. Therefore, stress decreases with increasing strain and reaches a minimum point. We can see very clear minimum points for D_0 = 24 and 30 μm and the value of minimum point decreases with decreasing D_0 value. When almost all the regions are filled with recrystallized grains ($\varepsilon \approx$ 0.25 - 0.30), stress increases again owing to the accumulation of dislocations in recrystallized grains. The second softening occurs after $\varepsilon \approx$ 0.25 and this cycle is repeated some times. Finally, the stresses for all D_0 values converge to almost the same values.

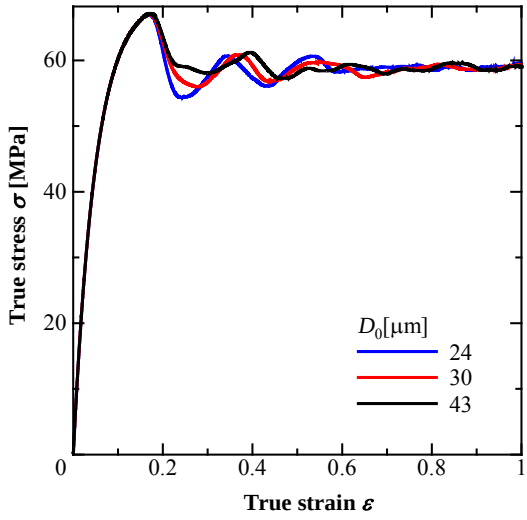

Fig. 4 Stress-strain curves.

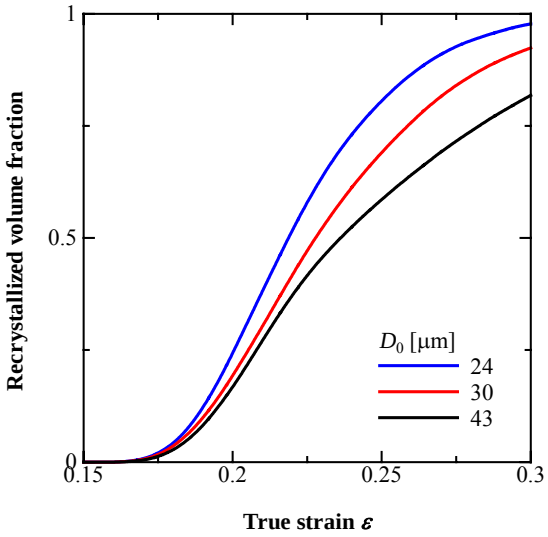

Fig. 5 Recrystallized volume fraction.

Figure 5 shows the variations in recrystallized volume fraction from $\varepsilon = 0.15$ to 0.30. It is observed that the recrystallization rate is higher for smaller initial grain sizes, since the area of the grain boundary that is the possible nucleation site increases with decreasing initial grain size D_0. Figure 6 shows the microstructural evolution from $\varepsilon = 0.15$ to 0.30. Recrystallized grains continuously nucleate on the grain boundaries and grow. Since recrystallized grains grow from the grain boundary to the center of the grains, the recrystallization rate is low for large initial grain sizes, as shown in Fig. 5. At $\varepsilon = 0.30$, almost all the regions are filled with recrystallized grains for $D_0 = 24$ μm. Figure 7 shows the variation in mean grain size D up to $\varepsilon = 0.50$. D is defined as $D = 2(A/\pi N)^{0.5}$, where N is the number of grains and A is the area of the computational domain. The amounts of D start from the initial grain size D_0 and decrease abruptly at the beginning of recrystallization. At the about $\varepsilon = 0.30$, the mean grain sizes for all D_0 values converge to almost the same values, $D \approx 10$ μm, although the stress-strain curves do not converge yet as shown in Fig. 4. Therefore, it is confirmed that the present model can reproduce the experimental fact that the mean grain size under the steady-state condition does not depend on initial grain size [4].

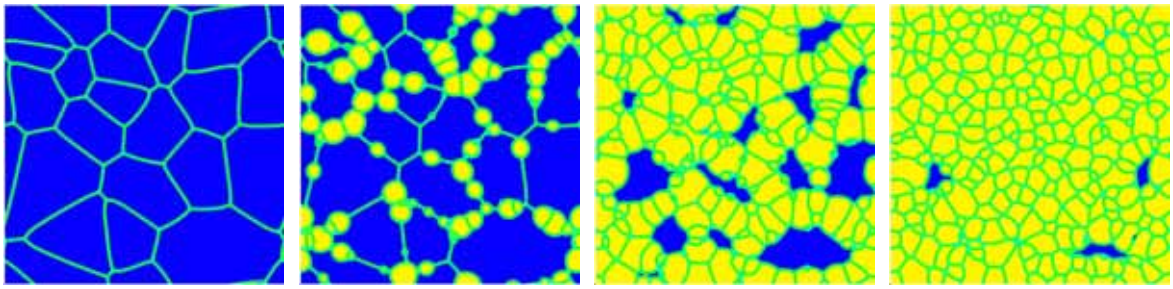

(a) D_0 = 24 μm

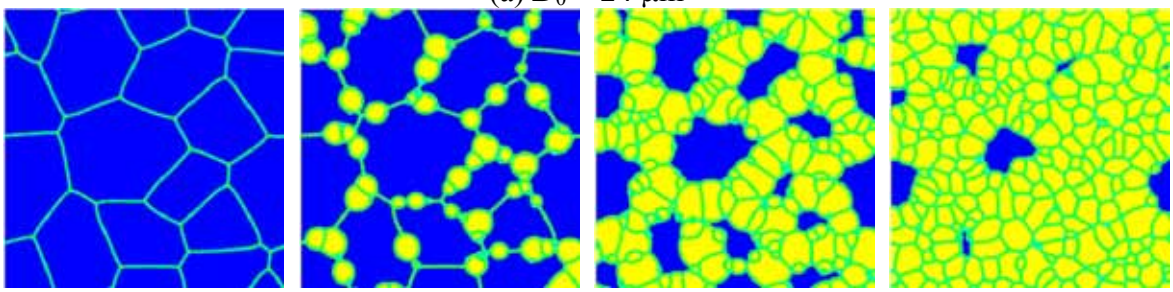

(b) D_0 = 30 μm

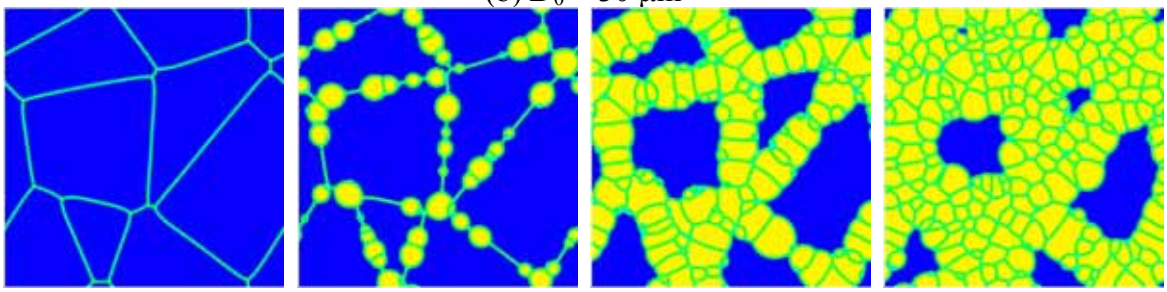

(c) D_0 = 43 μm

Fig. 6 Microstructures at ε = 0.15, 0.20, 0.25 and 0.30 from left.

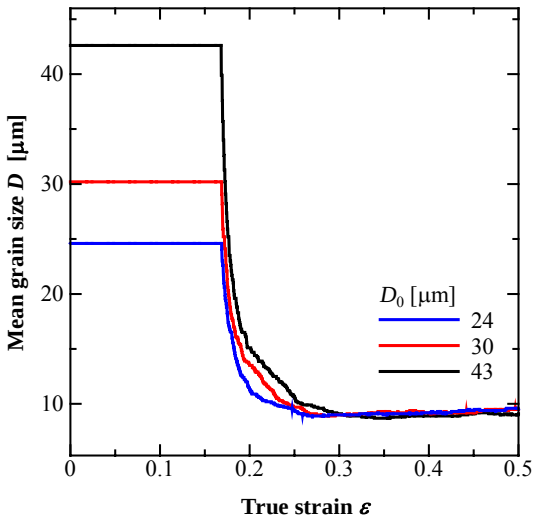

Figure. 7 Variation in mean grain size

2. Effects of inhomogeneous deformation In the present DRX model, deformation is perfectly homogeneous or dislocation densities are identical in all grains. However, in an actual material, deformation is inhomogeneous and localized. Here, we examine the dependences of inhomogeneous

deformation on DRX behavior. Inhomogeneous deformation is simply modeled by changing the initial dislocation density for every grain using $\rho_0 = \rho_0 \times 10^{5n}$, where ρ_0 is the initial dislocation density and n is a random number in the range of [0, 1]. The model with $D_0 = 43$ μm is employed here.

Figures 8 and 9 respectively show the stress-strain curves and microstructural evolution evaluated using the homogeneous and inhomogeneous deformation models. Since grains A, B, C and D in Fig. 9(b) have high initial dislocation densities, it is clear that DRX occurs at the grain boundaries. For the inhomogeneous model, DRX occurs at a smaller strain than that for the homogeneous model. As a result, the maximum stress decreases for the inhomogeneous model. From the above results, it is concluded that inhomogeneous or localized deformations induce early DRX. However, since the computational domain is relatively small, the differences in results between the homogeneous and inhomogeneous deformation models are small.

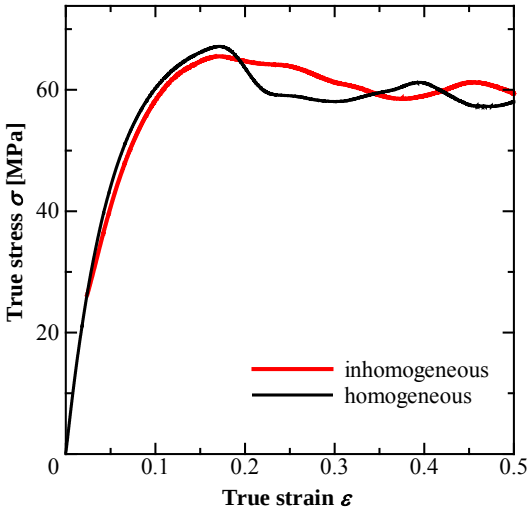

Figure. 8 Stress-strain curves for homogeneous and inhomogeneous deformations

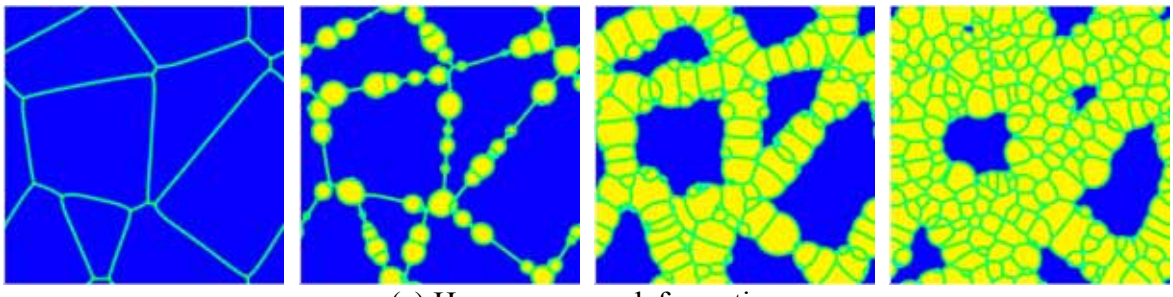

(a) Homogeneous deformation

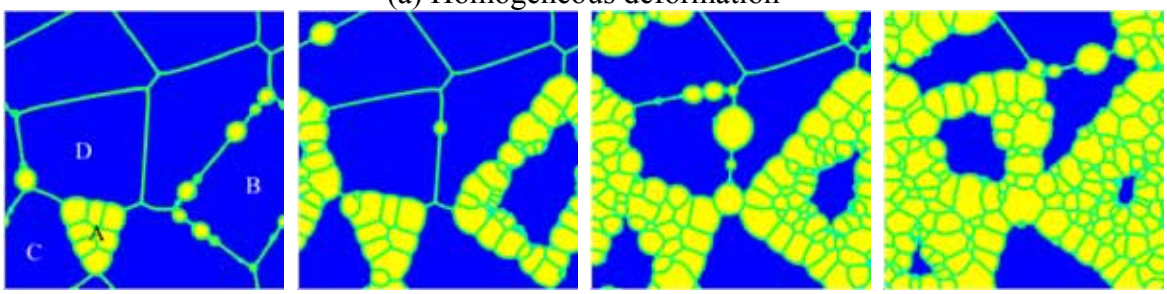

(b) Inhomogeneous deformation

Figure. 9 Microstructural evolutions for homogeneous and inhomogeneous deformations at ε = 0.15, 0.20, 0.25 and 0.30 from left.

CONCLUSIONS

The effects of initial grain size and the inhomogeneous deformation on the DRX behaviors are investigated by employing the phase-field method developed in our previous study. From the numerical results changing initial grain size, it has been clarified that maximum and minimum peak stresses at first cycle decreases with decreasing initial grain size, and the grain size in the final steady state doesn't depend on initial grain size. These numerical results are in good agreement with the experimental ones qualitatively. It is also observed that inhomogeneous or localized deformations induce early DRX.
Although this model is very simple DRX model, very important phenomena observed in DRX can be reproduced. Therefore, further investigations are possible using this DRX model to understand and predict DRX.

Acknowledgements Financial support from the Ministry of Education, Culture, Sports, Science and Technology of Japan through a Grant-in-Aid for Scientific Research is highly appreciated.

REFERENCES

[1] T. Takaki, A. Yamanaka, Y. Tomita, *Phase-Field Modeling for Dynamic Recrystallization*, *Proc. of International Conference on Advances and Trends in Engineering Materials and their Applications,* (2007) (*in press*).

[2] R. Ding, Z. X. Guo, *Coupled quantitative simulation of microstructural evolution and plastic flow during dynamic recrystallization*, Acta Mater., 49, (2001), 3163-3175.

[3] H. Mecking, U. F. Kocks, Acta Metall., 29, (1981), 1865-1875.

[4] T. Sakai, J. J. Jonas, *Dynamic recrystallization: Mechanical and microstructural considerations*, Acta Metall., 32, (1984), 189-209.

[5] W. Roberts, B. Ahlblom, *A nucleation criterion for dynamic recrystallization during hot working*, Acta Metal., 26, (1978), 801-813.

[6] I. Steinbach, F. Pezzolla, *A generalized field method for multiphase transformations using interface fields*, Physica D, 134, (1999), 385-393.